

Conformational analysis and stereochemical dependences of $^{31}\text{P}-^1\text{H}$ spin-spin coupling constants of bis(2-phenethyl)vinylphosphine and related phosphine chalcogenides

Sergey V. Fedorov, Leonid B. Krivdin,* Yury Yu. Rusakov, Igor A. Ushakov, Natalia V. Istomina, Natalia A. Belogorlova, Svetlana F. Malysheva, Nina K. Gusarova and Boris A. Trofimov

Theoretical energy-based conformational analysis of bis(2-phenethyl)vinylphosphine and related phosphine oxide, sulfide and selenide synthesized from available secondary phosphine chalcogenides and vinyl sulfoxides is performed at the MP2/6-311G** level to study stereochemical behavior of their $^{31}\text{P}-^1\text{H}$ spin-spin coupling constants measured experimentally and calculated at different levels of theory. All four title compounds are shown to exist in the equilibrium mixture of two conformers: major *planar s-cis* and minor *orthogonal* ones, while $^{31}\text{P}-^1\text{H}$ spin-spin coupling constants under study are found to demonstrate marked stereochemical dependences with respect to the geometry of the coupling pathways, and to the internal rotation of the vinyl group around the P(X)-C bonds (X = LP, O, S and Se), opening a new guide in the conformational studies of unsaturated phosphines and phosphine chalcogenides. Copyright © 2009 John Wiley & Sons, Ltd.

Keywords: NMR; $^{31}\text{P}-^1\text{H}$ spin-spin coupling constants; SOPPA; SOPPA(CCSD); conformational analysis; vinylphosphines; vinylphosphine chalcogenides

Introduction

Vinylphosphines and vinylphosphine chalcogenides are highly reactive building blocks which interact readily with different reagents (e.g. amines,^[1] phosphines^[2] and carbanion species^[3]) to afford functional phosphine chalcogenides. The latter are widely applied as hemilabile ligands for the design of advanced catalysts,^[4] flame retardants,^[5] extractants of rare earth and transuranic elements,^[6] and coordinating solvents for the synthesis of conductive nanomaterials.^[7] At the same time, known syntheses of vinylphosphines and vinylphosphine chalcogenides are based on hazardous phosphorus halides, vinyl derivatives of nontransition metals (such as Li, Mg, Sn), multistep, laborious and solvent-consuming procedures. Therefore, the development of facile methods for the preparation of unsaturated phosphines and phosphine chalcogenides represents an urgent synthetic challenge. One of the possible approaches to the synthesis of these compounds may involve the reaction of available vinyl sulfoxides^[8a] with bis(2-phenethyl)phosphine chalcogenides, easily prepared from red phosphorus and styrene in superbase systems.^[8b]

Apart from synthetic interest, vinylphosphines and related vinylphosphine chalcogenides are the attractive models for solving important theoretical problems, especially those dealing with stereochemical behavior of $^{31}\text{P}-^1\text{H}$ spin-spin coupling constants. In particular, very recently,^[9] the remarkable stereospecificity of $^2J(\text{Se},\text{H})$ and $^3J(\text{Se},\text{H})$ in divinyl selenide with respect to the internal rotation of both vinyl groups around the Se-C bonds has been reported to avoid possible caveats dealings with erroneous spectral assignments and misleading structural elucidations based

on $^{77}\text{Se}-^1\text{H}$ spin-spin coupling constants. It was thus a gratifying task to reveal if the same is true for $^2J(\text{P},\text{H})$ and $^3J(\text{P},\text{H})$ couplings involving the protons of the freely rotating vinyl groups in the series of vinylphosphines and related vinylphosphine chalcogenides under study.

Results and Discussion

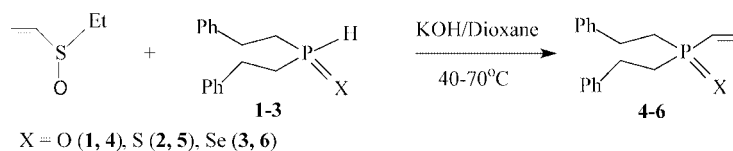
To obtain the desired set of vinylphosphine chalcogenides we have studied the reaction of ethyl vinyl sulfoxide with bis(2-phenethyl)phosphine chalcogenides **1-3**. The hydrophosphorylation proceeds in the system KOH-dioxane (40–70 °C) to give bis(2-phenethyl)vinylphosphine chalcogenides **4-6** in 87, 91 and 31% yields, correspondingly (Scheme 1).

Apparently, the reaction involves initial formation of adducts **7-9** (data of ^{31}P NMR), which further eliminate 1-ethanesulfenic acid to afford vinylphosphine chalcogenides **4-6** (Scheme 2).

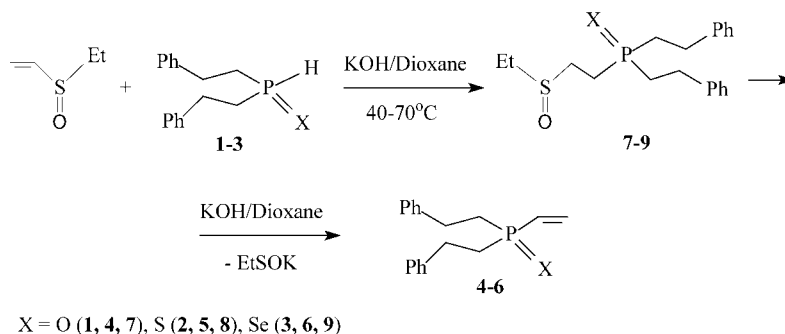
The corresponding bis(2-phenethyl)vinylphosphine (**10**) has been obtained from vinylphosphine sulfide **5** or vinylphosphine selenide **6** by their reduction under action of sodium in toluene (Scheme 3).

* Correspondence to: Leonid B. Krivdin, A. E. Favorsky Irkutsk Institute of Chemistry, Siberian Branch of the Russian Academy of Sciences, Favorsky St. 1, 664033 Irkutsk, Russia. E-mail: krivdin_office@irioch.irk.ru

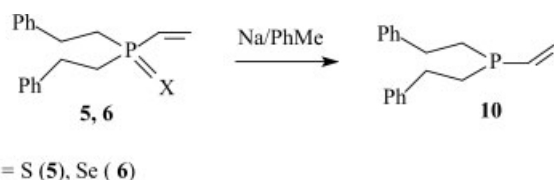
A. E. Favorsky Irkutsk Institute of Chemistry, Siberian Branch of the Russian Academy of Sciences, Favorsky St. 1, 664033 Irkutsk, Russia.



Scheme 1. Synthesis of bis(2-phenethyl)vinylphosphine chalcogenides **4-6**.



Scheme 2. Formation route of bis(2-phenethyl)vinylphosphine chalcogenides **4-6**.



Scheme 3. Synthesis of bis(2-phenethyl)vinylphosphine (**10**).

Prior to investigation of the stereochemical behavior of $^2J(\text{P,H})$ and $^3J(\text{P,H})$ couplings in the series of vinylphosphines and related vinylphosphine chalcogenides under study, theoretical conformational analysis of dimethylvinylphosphine (**11**) and three related phosphine chalcogenides (oxide, sulfide, and selenide) **12-14** has been carried out at the MP2/6-311G** level. As compared to the experimentally studied set of compounds, **4-6** and **10** in the model structures **11-14**, the methyl groups attached to the phosphorus atom were used instead of both phenethyl groups. Also, the same set of model compounds **11-14** was used further on in theoretical calculations of $^{31}\text{P}-^1\text{H}$ spin-spin coupling constants to be compared with experimental couplings in **4-6** and **10**.

Shown in Figs 1 and 2 are the rotational potential energy curves of **11-14** together with the corresponding probability density of population curves calculated on their basis. Full geometry optimizations were carried out at the MP2/6-311G** level in each rotational point of the potential energy curves incremented with 10 degrees step. Probability density of population curves were obtained from the numerical solution of the rotational Schrödinger equation using the finite difference method applied to the eigenvalues and eigenvectors problem of the corresponding second-order differential equations, and the resulting set of the found wavefunctions was averaged upon the calculated energy eigenvalues using the Maxwell-Boltzmann distribution at 300 K; potential energies used in the one-dimensional rotational Schrödinger equation were taken from the calculated potential energy curves and approximated by the Fourier series while the reduced moments of inertia were calculated from the optimized equilibrium geometries, as described in Ref. [10]. Traditionally,

in all calculations of probability density of population curves we used a well-approved MP2/6-311G** level of approximation taking into account electronic correlation effects within the second-order excitation theory and providing the most straightforward route to the high-accuracy energy-based conformational analysis.

Potential energy curves of all four studied compounds **11-14** (Figs 1(a,c) and 2(a,c)) display three minima corresponding to one *planar s-cis* conformer (A) and one twice-degenerated *orthogonal* conformer (B), and four maxima corresponding to two each twice-degenerated transition states (TS1 and TS2). Indeed, refining minimum search in the regions of the expected stationary points at the MP2/6-311G** level resulted in the localization of two true-minimum conformers (A and B) and two transition states (TS1 and TS2) for each of **11-14** shown in Figs 3 and 4. Harmonic frequencies analysis revealed no imaginary frequencies for the former (conformers) and showed one imaginary frequency for each of the latter (transition states). Numerical integration of the continuous probability density of population curves of **11-14** (Figs 1(b,d) and 2(b,d)) was used to determine the exact conformational ratio of the true-minimum conformers of **11-14** subject to their degeneracies (Table 1). We used these data further on for the conformational averaging of the calculated $^{31}\text{P}-^1\text{H}$ spin-spin coupling constants in **11-14**.

Results of this theoretical energy-based conformational analysis are generally in agreement with the available early^[11] and more recent^[12] theoretical and experimental data for the related compounds – unsaturated phosphines and phosphine chalcogenides – demonstrating predominance of the *planar s-cis* conformer in all cases, especially in phosphine chalcogenides as compared to phosphines. We will not address these results in more detail because data presented in Figs 1-4 and in Table 1 are to a great extent self-explanatory and require no further comments. Moreover, the goal of the present energy-based conformational analysis of **11-14** was not so much to perform it as itself as to provide for the further high-level *ab initio* study of the stereochemical behavior of $^{31}\text{P}-^1\text{H}$ spin-spin coupling constants involving protons of the vinyl group attached to the phosphorus atom bearing either lone pair (LP), as in **11**, or the sp^2 hybridized chalcogen atom (O, S and Se), as in **12-14**.

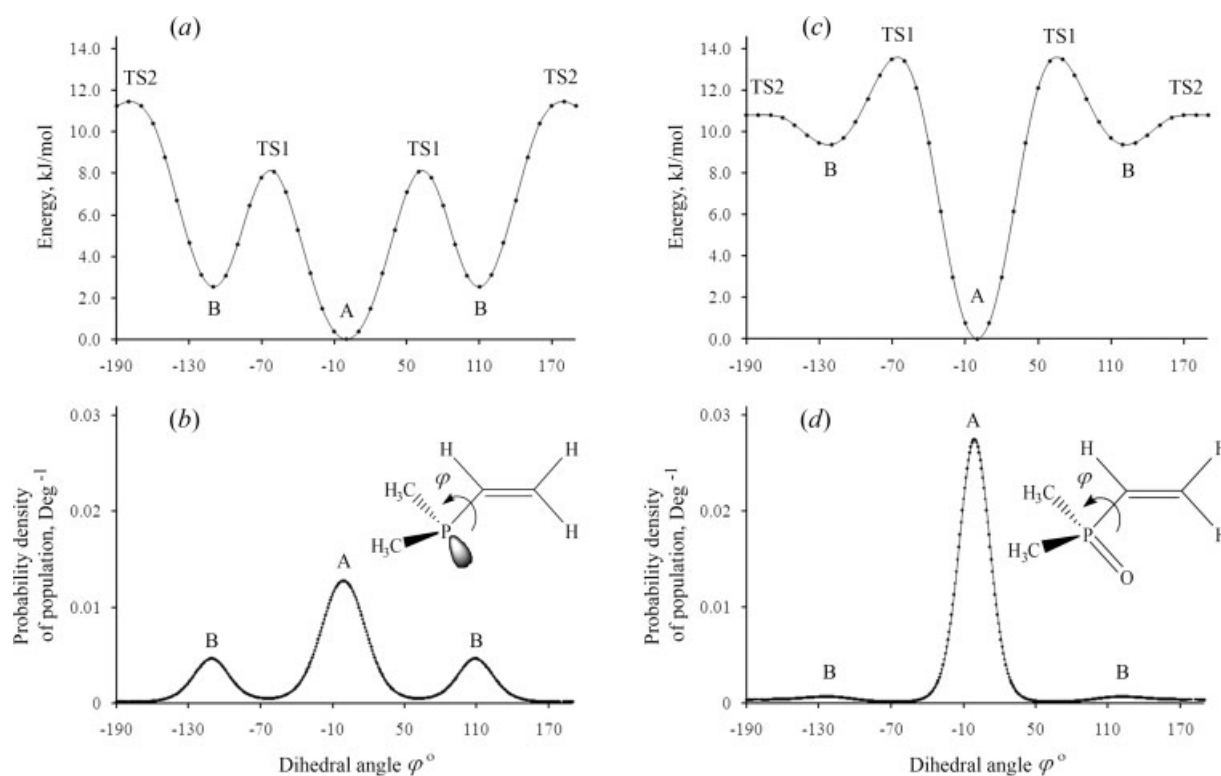


Figure 1. Rotational potential energy curves (a, c) and probability densities of population (b, d) of dimethylvinylphosphine (**11**) and dimethylvinylphosphine oxide (**12**) calculated at the MP2/6-311G** level. Values of $\varphi = 0^\circ$ are assigned to the *s-cis* arrangements of the vinyl group and either the phosphorus lone pair in **11** or the P=O bond in **12**, as shown.

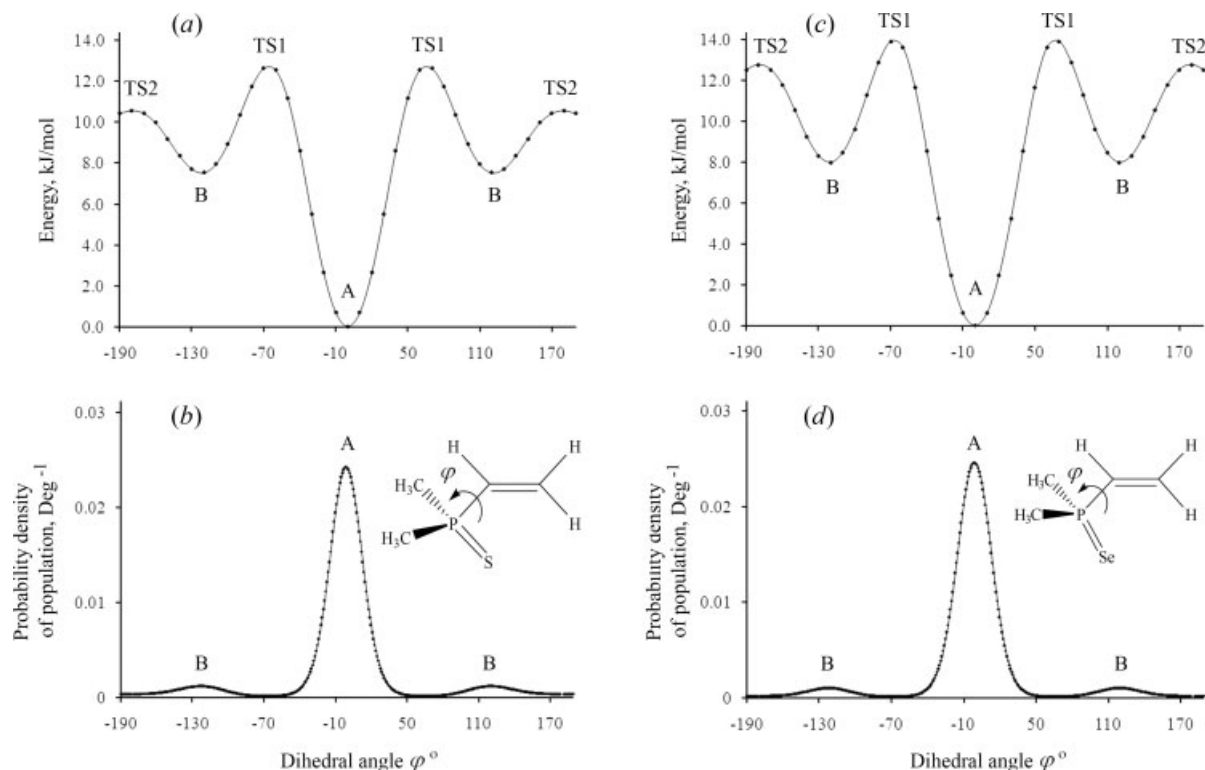


Figure 2. Rotational potential energy curves (a, c) and probability densities of population (b, d) of dimethylvinylphosphine sulfide (**13**) and dimethylvinylphosphine selenide (**14**) calculated at the MP2/6-311G** level. Values of $\varphi = 0^\circ$ are assigned to the *s-cis* arrangements of the vinyl group and the P=X bonds (X = S, Se), as shown.

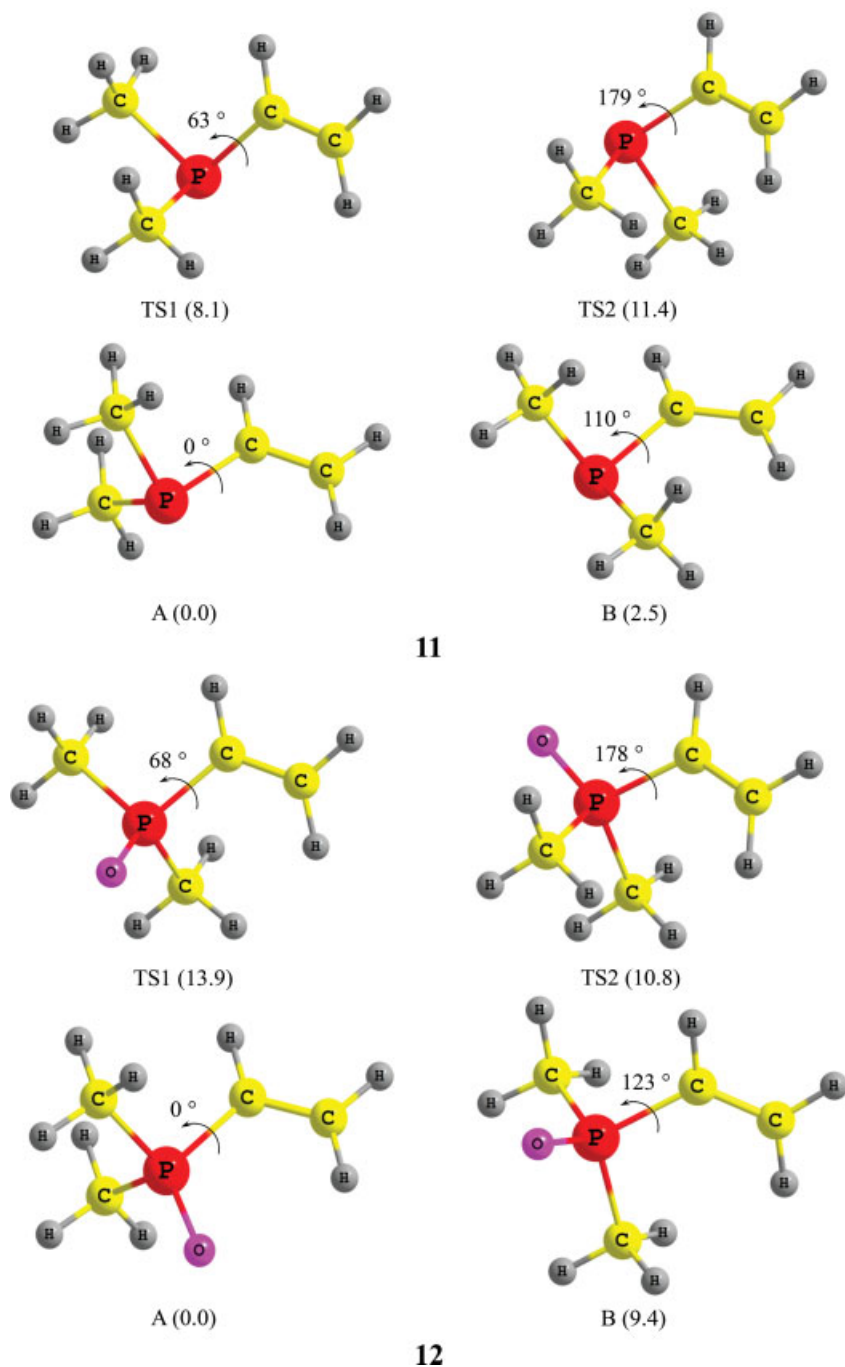


Figure 3. Equilibrium structures of the localized true-minimum conformers and transition states of dimethylvinylphosphine (**11**) and dimethylvinylphosphine oxide (**12**) optimized at the MP2/6-311G** level. Relative energies are given in parentheses (kJ/mol).

All $^{31}\text{P}-^1\text{H}$ spin-spin coupling constants have been calculated in **11–14** taking into account all four nonrelativistic coupling contributions to the total coupling, J : Fermi contact, J_{FC} , spin-dipolar, J_{SD} , diamagnetic spin-orbital, J_{DSO} , and paramagnetic spin-orbital, J_{PSO} , at three different levels of theory, namely within the DFT framework using the most popular Becke three-parameter hybrid functional^[13] with the Lee, Yang and Parr^[14] functional, B3LYP, and at the pure *ab initio* level using the second-order polarization propagator approach (SOPPA),^[15] and that in combination with the coupled cluster singles and doubles amplitudes approximation, SOPPA(CCSD).^[16] Four

different Dunning-type correlation-consistent basis sets have been used in all those calculations, namely double-zeta basis set augmented with inner correlation core *s*-functions, cc-pCVDZ,^[17] double- and triple-zeta basis sets of Dunning *et al.*^[18] with decontracted *s*-functions and augmented with two tight *s*-functions, accordingly, cc-pVDZ-su2 and cc-pVTZ-su2,^[19] and triple-zeta contracted basis set augmented with tight *s*-functions and optimized for calculation of spin-spin coupling constants, aug-cc-pVTZ-J.^[20] From our earlier experience (see, for example, recent review^[21] and references given therein), all these basis sets showed a rather good performance in calculations of spin-spin

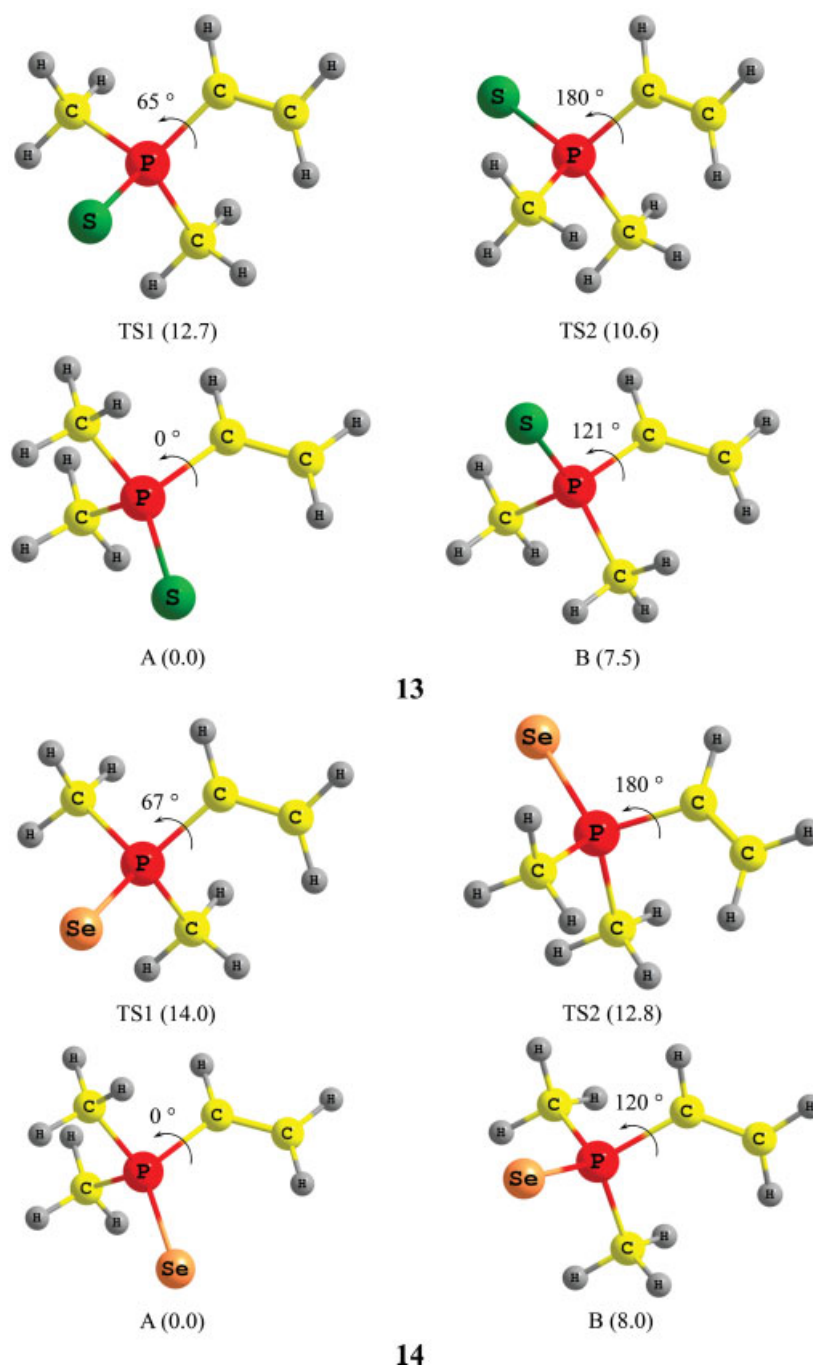


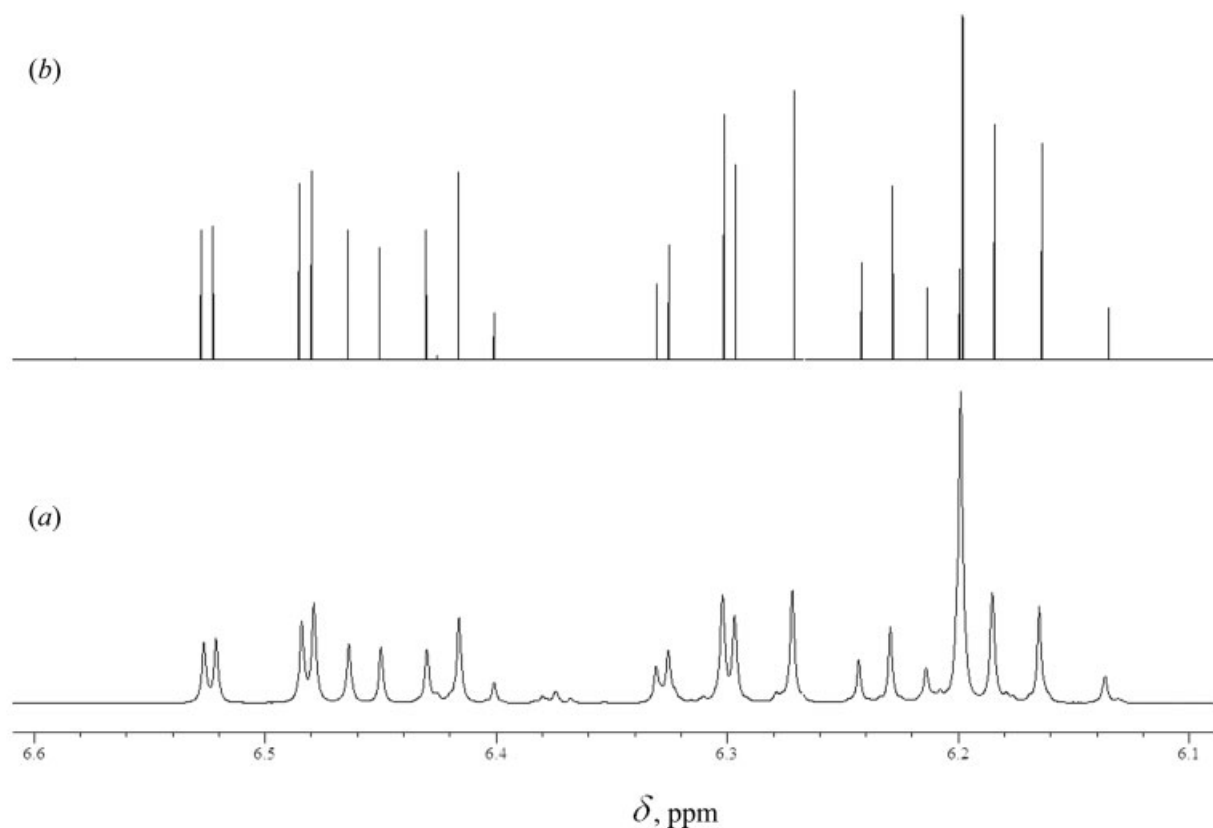
Figure 4. Equilibrium structures of the localized true-minimum conformers and transition states of dimethylvinylphosphine sulfide (**13**) and dimethylvinylphosphine selenide (**14**) optimized at the MP2/6-311G** level. Relative energies are given in parentheses (kJ/mol).

coupling constants of $^{13}\text{C}-^1\text{H}$, $^{13}\text{C}-^{13}\text{C}$ and $^{15}\text{N}-^1\text{H}$ types in a number of organic compounds at the SOPPA and DFT levels. As an example, the latter, aug-cc-pVTZ-J, was successfully employed very recently^[9] in the state-of-the-art SOPPA calculation of $^{77}\text{Se}-^1\text{H}$ couplings in divinyl selenide. So, the idea of the present study was to test these methods and title basis sets in the benchmark calculations of $^{31}\text{P}-^1\text{H}$ spin-spin coupling constants in the model dimethylvinylphosphine (**11**) and three related phosphine chalcogenides, **12–14**, in comparison with the experiment in the series of the four parent compounds, accordingly, **10** and **4–6**.

Experimental high-accuracy measurements of $^{31}\text{P}-^1\text{H}$ spin-spin coupling constants in **4–6** and **10** were carried out by the iterative high-order spectral analysis of the phosphorus-coupled ^1H NMR spectra, as illustrated in Fig. 5 for bis(phenethyl)vinylphosphine sulfide (**13**). Iterative spin simulations were performed in the framework of the four-spin systems ABCX representing the three-spin ABC patterns in the phosphorus-coupled ^1H NMR spectra of three protons of the vinyl groups (H_A , H_B and H_X) and X-parts (additionally coupled with four protons of two methylene groups) in the proton-coupled ^{31}P NMR spectra of **4–6** and **10**.

Table 1. True-minimum conformers and transition states of dimethylvinylphosphine (**11**) and dimethylvinylphosphine chalcogenides (**12–14**) localized at the MP2/6-311G** level

Cmpd	Conformation ^a	Type	Degeneracy	Population, ^b %	Relative energy, kJ/mol	Dihedral angle ϕ , Deg ^a	Imaginary frequency, cm ⁻¹
11	<i>planar s-cis</i> (A)	Conformer	1	61	0.0	0	–
	<i>orthogonal</i> (B)	Conformer	2	39	2.5	110	–
	TS1	Transition state	2	–	8.1	63	102.19
	TS2	Transition state	2	–	11.4	179	50.28
12	<i>planar s-cis</i> (A)	Conformer	1	91	0.0	0	–
	<i>orthogonal</i> (B)	Conformer	2	9	9.4	123	–
	TS1	Transition state	2	–	13.9	68	88.75
	TS2	Transition state	2	–	10.8	178	4.72
13	<i>planar s-cis</i> (A)	Conformer	1	85	0.0	0	–
	<i>orthogonal</i> (B)	Conformer	2	15	7.5	121	–
	TS1	Transition state	2	–	12.7	65	85.78
	TS2	Transition state	2	–	10.6	180	42.17
14	<i>planar s-cis</i> (A)	Conformer	1	90	0.0	0	–
	<i>orthogonal</i> (B)	Conformer	2	10	8.0	120	–
	TS1	Transition state	2	–	14.0	67	102.25
	TS2	Transition state	2	–	12.8	180	56.4

^a Shown in Figs 3 and 4.^b Data taken from the numerical integration of the probability density of population curves shown in Figs 1(b,d) and 2(b,d).**Figure 5.** Experimental (a) and simulated (b) phosphorus-coupled ¹H NMR spectra of bis(2-phenethyl)vinylphosphine sulfide (**5**) in CDCl₃ (161.98 MHz).

All ³¹P–¹H spin–spin coupling constants measured in **4–6** and **10** and calculated at different levels of theory in the related model compounds **11–14**, are compiled in Table 2. First of all, it should be noted that generally, rather good results are obtained at all levels of theory, with SOPPA and SOPPA(CCSD) performing

noticeably better than DFT-B3LYP. It is noteworthy that the more time-consuming SOPPA(CCSD) method shows no appreciable improvement as compared to SOPPA. Especially, very good results are obtained at the SOPPA level when using aug-cc-pVTZ-J basis set of Sauer *et al.*^[20] Comparing basis set performance, it also

Table 2. $^{31}\text{P}-^1\text{H}$ Spin-spin coupling constants of dimethylvinylphosphine (**11**) and dimethylvinylphosphine chalcogenides (**12–14**) calculated at different levels of theory^a

Cmpd	spin-spin coupling constant ^b	Method	Basis set				Experiment	
			cc-pCVDZ	cc-pVDZ-su2	cc-pVTZ-su2	aug-cc-pVTZ-J		
11	$^2J(\text{P},\text{H}_\text{X})$	DFT-B3LYP	7.3	11.7	11.9	4.0	5.8 ^c	
		SOPPA	2.0	5.0	5.1	5.2		
		SOPPA(CCSD)	2.2	5.2	5.3	5.2		
	$^3J(\text{P},\text{H}_\text{A})$	DFT-B3LYP	24.6	28.4	29.2	29.9		30.4 ^c
		SOPPA	26.4	28.8	29.1	29.7		
		SOPPA(CCSD)	24.8	27.1	27.4	28.0		
	$^3J(\text{P},\text{H}_\text{B})$	DFT-B3LYP	11.0	13.2	13.8	14.3		13.1 ^c
		SOPPA	12.8	14.4	14.6	15.0		
		SOPPA(CCSD)	12.1	13.6	13.8	14.2		
12	$^2J(\text{P},\text{H}_\text{X})$	DFT-B3LYP	21.7	32.2	33.6	35.8	28.0 ^d	
		SOPPA	13.7	20.3	21.6	23.7		
		SOPPA(CCSD)	14.3	20.9	22.1	24.0		
	$^3J(\text{P},\text{H}_\text{A})$	DFT-B3LYP	31.3	35.8	36.2	37.0		37.9 ^d
		SOPPA	33.2	35.7	35.4	36.3		
		SOPPA(CCSD)	31.0	33.4	33.2	33.9		
	$^3J(\text{P},\text{H}_\text{B})$	DFT-B3LYP	17.6	21.3	21.7	22.2		20.8 ^d
		SOPPA	19.5	20.0	21.6	22.2		
		SOPPA(CCSD)	17.9	20.3	20.1	20.6		
13	$^2J(\text{P},\text{H}_\text{X})$	DFT-B3LYP	21.5	30.2	30.8	32.3	26.8 ^e	
		SOPPA	12.9	17.9	14.4	19.9		
		SOPPA(CCSD)	13.3	18.3	18.7	20.1		
	$^3J(\text{P},\text{H}_\text{A})$	DFT-B3LYP	37.1	43.0	43.5	44.5		44.0 ^e
		SOPPA	38.8	42.4	44.0	43.1		
		SOPPA(CCSD)	36.2	39.6	39.3	40.2		
	$^3J(\text{P},\text{H}_\text{B})$	DFT-B3LYP	21.0	25.5	25.7	26.4		24.4 ^e
		SOPPA	23.0	25.7	27.7	25.8		
		SOPPA(CCSD)	21.2	23.8	23.3	23.9		
14	$^2J(\text{P},\text{H}_\text{X})$	DFT-B3LYP	24.1	33.7	33.2	33.6	24.6 ^f	
		SOPPA	14.2	19.4	16.9	17.7		
		SOPPA(CCSD)	14.7	19.9	17.2	17.9		
	$^3J(\text{P},\text{H}_\text{A})$	DFT-B3LYP	40.0	46.4	46.7	47.6		45.4 ^f
		SOPPA	41.4	45.2	47.2	48.2		
		SOPPA(CCSD)	38.6	42.3	43.6	44.5		
	$^3J(\text{P},\text{H}_\text{B})$	DFT-B3LYP	23.2	28.1	28.1	28.5		25.2 ^f
		SOPPA	24.7	27.7	30.0	30.6		
		SOPPA(CCSD)	22.8	25.6	27.6	28.1		

^a All couplings in Hz.^b Conformationally averaged as described in the text.^c Measured in cmpd. **10**.^d Measured in cmpd. **4**.^e Measured in cmpd. **5**.^f Measured in cmpd. **6**.

becomes apparent that double- as well as triple-zeta sets with decontracted *s*-functions, cc-pVXZ-su2 (*X* = D, T), show almost equally good results while double-zeta basis set augmented with inner correlation core *s*-functions, cc-pCVDZ, performs noticeably worse. It is thus SOPPA/aug-cc-pVTZ-J level which we will use further on in the calculations of $^{31}\text{P}-^1\text{H}$ coupling constants.

Interestingly, vicinal $^{31}\text{P}-^1\text{H}$ spin-spin coupling constants, $^3J(\text{P},\text{H})$, are more gratifying objects for theoretical calculations as compared to geminal couplings, $^2J(\text{P},\text{H})$. For the latter, in the series of vinylphosphine chalcogenides **12–14**, DFT-B3LYP method unacceptably overestimates experimental $^2J(\text{P},\text{H})$ values by ca

6–9 Hz while SOPPA and SOPPA(CCSD) essentially underestimates experimental $^2J(\text{P},\text{H})$ couplings by ca 4–6 Hz. At the same time, both vicinal couplings, $^3J(\text{P},\text{H}_\text{A})$ and $^3J(\text{P},\text{H}_\text{B})$, are reproduced at all levels of theory with a good accuracy of ca 2 Hz.

It is noteworthy that a good agreement of calculated $^{31}\text{P}-^1\text{H}$ spin-spin coupling constants in **11–14** with experiment is achieved only provided the conformational averaging of the former is applied. In fact, theoretical value of each $J(\text{P},\text{H})$ coupling given in Table 2 is obtained by its conformational averaging between the true-minimum conformers of **11–14** (*i.e.* calculated in both true-minimum conformers of each compound and averaged

Table 3. $^{31}\text{P}-^1\text{H}$ Spin–spin coupling constants in different conformers of dimethylvinylphosphine (**11**) and dimethylvinylphosphine chalcogenides (**12–14**) calculated at the SOPPA/aug-cc-pVTZ-J level of theory ^{a)}

Cmpd	spin–spin coupling constant	Conformer ^b	Calculated					Experiment
			J_{dso}	J_{pso}	J_{sd}	J_{fc}	J	
11	$^2J(\text{P},\text{H}_\text{X})$	<i>planar s-cis</i> (A)	−0.3	−0.7	−0.3	−9.7	−11.0	5.8 ^c
		<i>orthogonal</i> (B)	−0.3	−0.8	0.0	31.5	30.4	
	$^3J(\text{P},\text{H}_\text{A})$	<i>planar s-cis</i> (A)	−0.6	0.0	−0.1	40.3	39.6	30.4 ^c
		<i>orthogonal</i> (B)	−0.6	0.1	0.2	14.4	14.2	
	$^3J(\text{P},\text{H}_\text{B})$	<i>planar s-cis</i> (A)	0.1	−0.5	0.1	19.9	19.5	13.1 ^c
		<i>orthogonal</i> (B)	−0.1	−0.0	−0.2	8.4	8.1	
12	$^2J(\text{P},\text{H}_\text{X})$	<i>planar s-cis</i> (A)	−0.1	−0.3	−0.0	25.8	25.3	28.0 ^d
		<i>orthogonal</i> (B)	−0.1	−0.4	−0.0	8.5	8.0	
	$^3J(\text{P},\text{H}_\text{A})$	<i>planar s-cis</i> (A)	−0.5	0.3	−0.1	36.3	36.0	37.9 ^d
		<i>orthogonal</i> (B)	−0.5	0.4	−0.0	39.6	39.4	
	$^3J(\text{P},\text{H}_\text{B})$	<i>planar s-cis</i> (A)	0.2	−0.3	−0.1	22.5	22.3	20.8 ^d
		<i>orthogonal</i> (B)	0.1	−0.0	−0.1	20.8	20.8	
13	$^2J(\text{P},\text{H}_\text{X})$	<i>planar s-cis</i> (A)	−0.1	−0.4	−0.1	21.6	21.0	26.8 ^e
		<i>orthogonal</i> (B)	−0.0	−0.5	−0.0	14.4	13.9	
	$^3J(\text{P},\text{H}_\text{A})$	<i>planar s-cis</i> (A)	−0.5	0.3	−0.0	43.6	43.4	44.0 ^e
		<i>orthogonal</i> (B)	−0.5	0.4	0.0	41.5	41.4	
	$^3J(\text{P},\text{H}_\text{B})$	<i>planar s-cis</i> (A)	0.2	−0.2	−0.1	26.5	26.4	24.4 ^e
		<i>orthogonal</i> (B)	0.1	−0.0	−0.1	22.5	22.5	
14	$^2J(\text{P},\text{H}_\text{X})$	<i>planar s-cis</i> (A)	0.1	−0.5	−0.2	18.9	18.3	24.6 ^f
		<i>orthogonal</i> (B)	0.1	−0.5	−0.1	13.5	13.0	
	$^3J(\text{P},\text{H}_\text{A})$	<i>planar s-cis</i> (A)	−0.4	0.2	−0.1	48.8	48.5	45.4 ^f
		<i>orthogonal</i> (B)	−0.4	0.2	−0.1	46.0	45.7	
	$^3J(\text{P},\text{H}_\text{B})$	<i>planar s-cis</i> (A)	0.4	−0.2	−0.1	31.0	31.1	25.2 ^f
		<i>orthogonal</i> (B)	0.3	−0.0	−0.1	26.3	26.5	

^a All couplings and coupling contributions in Hz.
^b Optimized at the MP2/6-311G** level, see Figs 3 and 4.
^c Measured in compd. **10**.
^d Measured in compd. **4**.
^e Measured in compd. **5**.
^f Measured in compd. **6**.

according to their populations subject to their degeneracies). Given in Table 3 are the $^{31}\text{P}-^1\text{H}$ spin–spin coupling constants calculated in different conformers of **11–14**. According to these data, it appears that conformational averaging is a crucial point in theoretical calculations of $J(\text{P},\text{H})$ in vinylphosphines and vinylphosphine chalcogenides. Indeed, all geminal couplings, $^2J(\text{P},\text{H}_\text{X})$, differ dramatically in *planar s-cis* and *orthogonal* conformers of **11–14**, and the same is true for both vicinal couplings, $^3J(\text{P},\text{H}_\text{A})$ and $^3J(\text{P},\text{H}_\text{B})$, in vinylphosphine **11**, see Table 3. For example, $^2J(\text{P},\text{H}_\text{X})$ is ca −11 Hz in *planar s-cis* conformer of **11**, while it is more than +30 Hz in its *orthogonal* conformation. On the other hand, the values of $^3J(\text{P},\text{H}_\text{A})$ in the title conformers of **11** totals to accordingly, ca +40 and +14 Hz. Needless to recall that this remarkable stereospecificity of all studied $J(\text{P},\text{H})$ is provided by their Fermi contact contributions, as it follows from the data presented in Table 3.

Additional calculations were performed to evaluate the effect of the replacement of two phenethyl substituents by the methyl groups on calculated spin–spin couplings. For this purpose, *planar s-cis* and *orthogonal* conformers of bis(2-phenethylvinyl)phosphine (**10**) were localized at the MP2/6-311G** level, and all three conformationally averaged $^{31}\text{P}-^1\text{H}$ spin–spin coupling constants were calculated at the highest possible level B3LYP/6-31G* (restricted by molecular size and

software limitations) to be compared with the corresponding data for the model dimethylvinylphosphine (**11**) obtained under equivalent conditions. It appeared that the replacement of two phenethyl substituents by the methyl groups on going from **10** to **11** provides no noticeable effect on the calculated $^{31}\text{P}-^1\text{H}$ spin–spin coupling constants (varying from 0.5 to 1 Hz), either on their total values or their individual contributions, which justifies the usage of compounds **11–14** as molecular models for, accordingly, **10** and **4–6**.

This striking evidence of apparent very strong conformational behavior of $J(\text{P},\text{H})$ in vinylphosphines and vinylphosphine chalcogenides encouraged us to study their dihedral angle dependences in the series of model set of **11–14**, and the most interesting results are depicted in Figs 6–8.

The most remarkable dihedral angle dependences are found for all three $^{31}\text{P}-^1\text{H}$ spin–spin couplings, $^2J(\text{P},\text{H}_\text{X})$, $^3J(\text{P},\text{H}_\text{A})$ and $^3J(\text{P},\text{H}_\text{B})$, in vinylphosphine **11** (Fig. 6) which is not surprising and should be accounted for the well known LP effect upon spin–spin coupling constants of different types reviewed by Gil and Phillipsborn.^[22] Indeed, when going from *s-cis* ($\phi = 0^\circ$) to *s-trans* ($\phi = 180^\circ$) conformation of **11** (notation of ϕ in **11** is given in Fig. 1), one should expect the increase of $^2J(\text{P},\text{H}_\text{X})$ and decrease of $^3J(\text{P},\text{H}_\text{A})$ and $^3J(\text{P},\text{H}_\text{B})$ – that is what we expected and what we

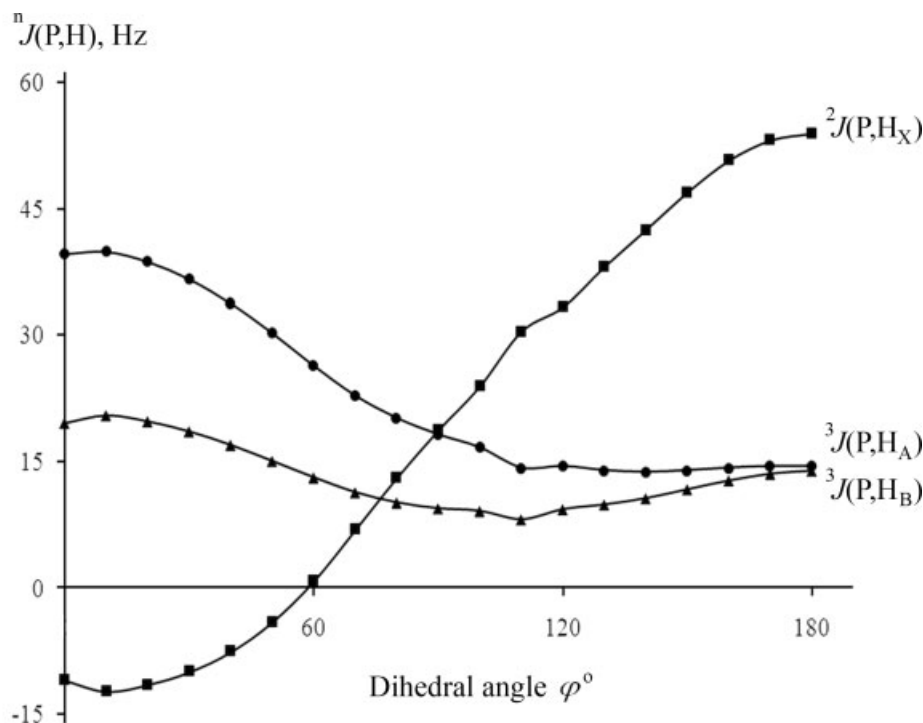


Figure 6. Dihedral angle dependences of ${}^2J(\text{P,H})$ and ${}^3J(\text{P,H})$ in dimethylvinylphosphine (**11**) calculated at the SOPPA level. Values of $\phi = 0^\circ$ are assigned to the *s-cis* arrangements of the vinyl group and the phosphorus lone pair.

see in Fig. 6. For example, ${}^2J(\text{P,H}_X)$ increases by more than 60 Hz (!) when going from *s-cis* to *s-trans* conformation which is due to the hyperconjugative $n_\sigma - \sigma_{\text{CH}}^*$ interaction involving phosphorus LP and antibonding orbital of the C-H_X bond (the so-called *Perlin effect* or a particular case of anomeric effect^[23]) in *s-cis* conformation resulting in the marked decrease of ${}^2J(\text{P,H}_X)$. On the other hand, spatial proximity of phosphorus LP and one of the coupled nuclei, H_X, in the *s-trans* conformation results in the marked increase of ${}^2J(\text{P,H}_X)$. It is the interplay of these two effects which results in the dramatic difference of more than 60 Hz of this coupling in *s-cis* and *s-trans* conformations of **11**. The same remarkable stereospecificity of ${}^2J(\text{Se,H})$ and ${}^3J(\text{Se,H})$ involving protons of the vinyl group attached to selenium atom due to the orientational LP effect of selenium was documented very recently⁹ for divinyl selenide.

Turning to vinylphosphine chalcogenides **12–14**, it should be noted that ${}^2J(\text{P,H}_X)$ increases by *ca* 4 Hz in **12** while it decreases by *ca* 9 Hz in **13** and by *ca* 5 Hz in **14** when going from *s-cis* ($\phi = 0^\circ$) to *s-trans* ($\phi = 180^\circ$) conformations of **12–14** (notations of ϕ in **12–14** are given in Figs 1 and 2), see Fig. 7. Conformational effects on vicinal couplings, ${}^3J(\text{P,H}_A)$ and ${}^3J(\text{P,H}_B)$, are much less pronounced in this series (within the range of $\Delta J \approx 2$ Hz), except for ${}^3J(\text{P,H}_B)$ in vinylphosphine oxide **12**, the latter markedly decreasing by *ca* 20 Hz with ϕ increasing from 0 to 180° (Fig. 8). We will not address these effects in detail which are apparently due to the particular hyperconjugative interactions involving the P=X double bonds ($X = \text{O}, \text{S}, \text{Se}$) which are above the scope of the present communication and which deserve the special detailed studies like those done in several recent publications by *Contreras* and colleagues.^[24]

Concluding Remarks

A detailed study of the conformational behavior of geminal and vicinal ${}^{31}\text{P}-{}^1\text{H}$ spin–spin coupling constants in the series of vinylphosphine and vinylphosphine chalcogenides has been performed at different levels of theory in comparison with experiment. The most interesting result of this communication is that ${}^{31}\text{P}-{}^1\text{H}$ couplings provide very marked stereospecificity with respect to the orientational phosphorus LP effect and that of the P=X double bonds ($X = \text{O}, \text{S}, \text{Se}$) which implies a great care to be taken in the stereochemical studies of unsaturated phosphines and phosphine chalcogenides based on ${}^{31}\text{P}-{}^1\text{H}$ spin–spin coupling constants. To avoid misleading conclusions and erroneous spectral assignments based on ${}^2J(\text{P,H})$ and ${}^3J(\text{P,H})$, the trends of their stereochemical behavior reported herewith should first be taken into account before any of their conformational applications.

Experimental

NMR measurements

${}^1\text{H}$, ${}^{13}\text{C}$, and ${}^{31}\text{P}$ NMR spectra were recorded on a Bruker DPX 400 MHz spectrometer (${}^1\text{H}$, 400.13 MHz; ${}^{13}\text{C}$, 100.62 MHz; ${}^{31}\text{P}$, 161.98 MHz) in a 5 mm broadband probe at 25°C in CDCl_3 with HMDS (hexamethyldisiloxane) as an internal standard. ${}^{31}\text{P}-{}^1\text{H}$ coupling constants were measured from the phosphorus-coupled ${}^1\text{H}$ NMR spectra using the spectral settings as follows: 90° pulse length, 7 μs ; spectral width, 4 kHz; acquisition time, 5 s; relaxation delay, 10 s; spectral resolution 0.05 Hz/pt; accumulation time, 10 min.

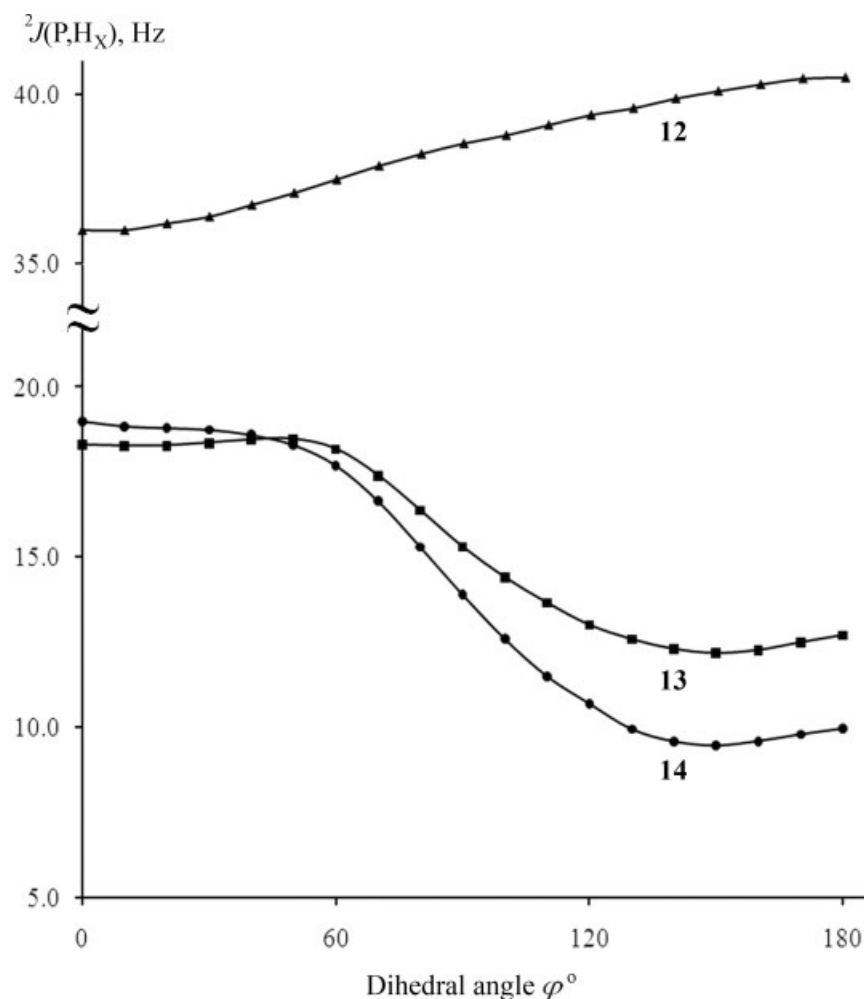


Figure 7. Dihedral angle dependences of ${}^2J(\text{P},\text{H})$ in dimethylvinylphosphine chalcogenides (**12–14**) calculated at the SOPPA level. Values of $\phi = 0^\circ$ are assigned to the *s-cis* arrangements of the vinyl group and the $\text{P}=\text{X}$ bonds ($\text{X} = \text{O}, \text{S}, \text{Se}$).

Computational details

All geometry optimizations and calculations of the potential energy curves of **11–14** were performed with the GAMESS code^[25] at the MP2 perturbation level using the 6-311G** basis set of Pople and coworkers^[26] without symmetry constraints, i.e. assuming the C_1 symmetry point group. Calculations of spin–spin coupling constants have been carried out taking into account all four nonrelativistic coupling contributions with the DALTON package^[27] at the DFT-B3LYP, SOPPA, and SOPPA(CCSD) levels with different basis sets discussed in the text using the stationary equilibrium MP2/6-311G** geometries.

Synthesis

Synthesis of vinylphosphine chalcogenides 4–6. Suspension of ethyl vinyl sulfoxide, phosphine chalcogenides **1–3** (molar ratio $\sim 1:1$) and KOH in dioxane was heated at $40\text{--}70^\circ\text{C}$. The resulted suspension was filtrated, dioxane was removed from the filtrate to give phosphine chalcogenides **4–6** (details of the experiments will be published later).

Bis(2-phenethyl)vinylphosphine oxide (4). Colourless crystals, mp 92°C (acetone); IR (KBr, cm^{-1}): 465, 492 (δ , CPC), 698 [δ , CH(Ph)], 756 (ν , P-C), 781 [δ , CH(Ph)], 834 (ω , =CH₂), 942, 965 (τ , =CH),

1009, 1141 [δ , CH(Ph)], 1167 (ν , P=O), 1213 [δ , CH(Ph)], 1390 (δ , =CH₂), 1453 (δ , CH₂), 1497, 1583, [ν , C=C(Ph)], 1603 [ν , C=C (C=C), C=C(Ph)], 2853, 2863, 2922, 2997 (ν , CH), 3001, 3027, 3062, 3085, 3106 [ν , =CH₂, =CH (C=C), C=C(Ph)]; ${}^1\text{H}$ chemical shifts, CDCl_3 (δ , ppm): 1.99–2.11 (m, 4H, CH₂ P=O); 2.86–2.94 (m, 4H, CH₂Ph); 6.14 (m, 1H, H(X)); 6.25 (m, 1H, H(A)); 6.38 (m, 1H, H(B)); 7.18–7.28 (m, 10H, Ph); ${}^2J_{\text{H(A)H(B)}} = 1.4$ Hz; ${}^3J_{\text{H(A)H(X)}} = 12.6$ Hz; ${}^3J_{\text{H(B)H(X)}} = 18.5$ Hz; ${}^2J_{\text{PH(X)}} = 28.0$ Hz; ${}^3J_{\text{PH(A)}} = 37.9$ Hz; ${}^3J_{\text{PH(B)}} = 20.8$ Hz; ${}^{13}\text{C}$ chemical shifts, CDCl_3 , (δ , ppm): 27.60 (M (CPh), ${}^2J_{\text{PC}} = 3.0$ Hz), 31.60 (CP, ${}^1J_{\text{PC}} = 67.0$ Hz), 126.50 (C_p), 128.10 (C_o), 128.70 (C_m), 130.70 (=CH₂, ${}^1J_{\text{PC}} = 86.8$ Hz), 135.20 (=CH), 141.0 (C_{ipso}, ${}^3J_{\text{PC}} = 14.1$ Hz); ${}^{31}\text{P}$ chemical shifts, CDCl_3 , (δ , ppm): 36.0. Calc. for $\text{C}_{18}\text{H}_{21}\text{OP}$ (%): C, 76.04; H, 7.44; P, 10.89. Found (%): C, 75.35; H, 7.24; P, 9.93.

Bis(2-phenethyl)vinylphosphine sulfide (5). Light-yellow oil; IR (cm^{-1}): 472, 495 (δ , CPC), 543 (ν , P=S), 698 [δ , CH(Ph)], 749 (ν , P-C), 767 [δ , CH(Ph)], 831, 842 (ω , =CH₂); 946, 980 (τ , =CH), 1012, 1134, 1181, 1211 [δ , CH(Ph)], 1384 (δ , =CH₂), 1453 (δ , =CH₂), 1496, 1584, 1602 [ν , C=C(Ph)]; 2862, 2892, 2929 (ν , CH), 3000, 3026, 3061, 3084, 3103 [ν , =CH(Ph)]; ${}^1\text{H}$ chemical shifts, CDCl_3 (δ , ppm): 2.13–2.28 (m, 4H, CH₂P); 2.79–3.06 (m, 4H, CH₂Ph); 6.22 (m, 1H, H(X)); 6.25 (m, 1H, H(A)); 6.47 (m, 1H, H(B)); 7.20–7.33 (m, 10H, Ph); ${}^2J_{\text{H(A)H(B)}} = 1.6$ Hz, ${}^3J_{\text{H(A)H(X)}} = 11.5$ Hz, ${}^3J_{\text{H(B)H(X)}} = 17.6$ Hz. ${}^2J_{\text{PH(X)}} = 26.8$ Hz, ${}^3J_{\text{PH(A)}} = 44.0$ Hz, ${}^3J_{\text{PH(B)}} = 24.4$ Hz; ${}^{13}\text{C}$ chemical shifts, CDCl_3 , (δ , ppm): 28.30 (d, CPh, ${}^2J_{\text{PC}} = 2.1$ Hz), 34.20 (d, CP, ${}^1J_{\text{PC}} =$

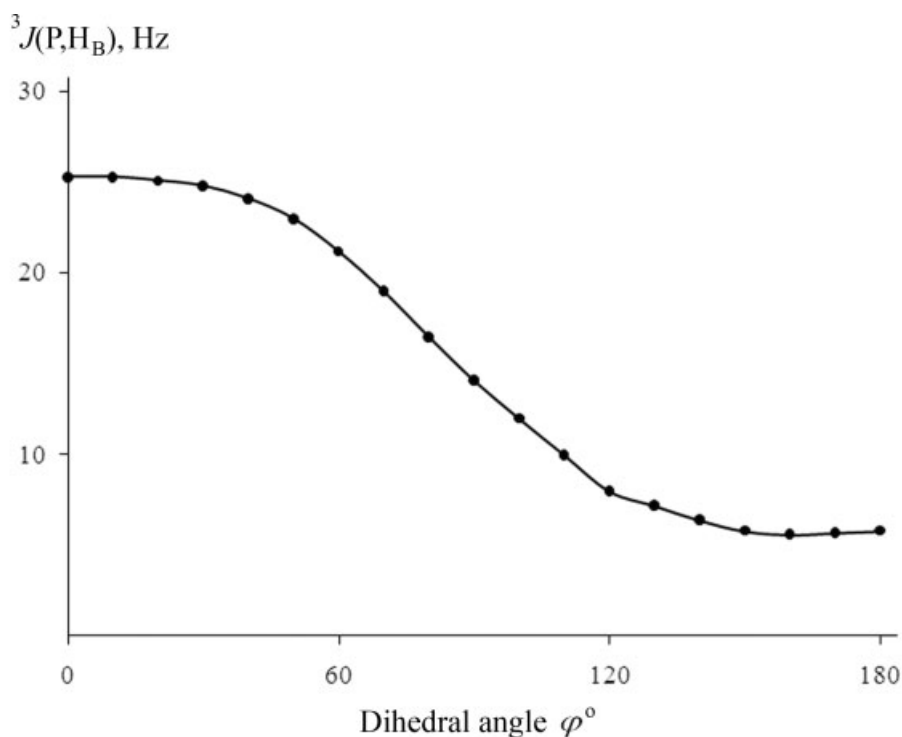


Figure 8. Dihedral angle dependence of $^3J(P,H_B)$ in dimethylvinylphosphine oxide (**12**) calculated at the SOPPA level. Value of $\phi = 0^\circ$ is assigned to the *s-cis* arrangement of the vinyl group and the P=O bond.

52.8 Hz), 126.50 (C_p), 128.30 (C_o), 128.70 (C_m), 130.10 (d, $CH_2 =$, $^1J_{PC} = 69.9$ Hz), 135.20 (d, $=CH$, $^2J_{PC} = 1.1$ Hz), 140.8 (d, C_{ipso} , $^3J_{PC} = 15.1$ Hz); ^{31}P chemical shifts, $CDCl_3$, (δ , ppm): 42.52. Calc. for $C_{18}H_{21}PS$ (%): C, 71.97; H, 7.05; P, 10.31, S, 10.67. Found (%): C, 71.82; H, 6.99; P, 10.91, S, 10.51.

Bis(2-phenethylvinyl)phosphine selenide (6). Light-yellow oil; IR (cm^{-1}): 448 (ν , P=Se), *shl* 465, 493 (δ , CPC), 698 [δ , CH(Ph)], 753 (ν , P-C), 769 (δ , CH of phenyl rings), 839, 860 (ω , $=CH_2$), 945, 978 (τ , $=CH$), 1013, 1134, 1210 [δ , CH(Ph)], 1382 (δ , $=CH_2$), 1453 (δ , CH_2), 1496, 1583 [ν , C=C(Ph)], 1602 [ν , C=C (C=C), C=C(Ph)], 2863, 2903, 2926, 2946 (ν , CH), 3001, 3026, 3061, 3084, 3106 [ν , $=CH_2$, $=CH$ (C=C), C=C(Ph)]; 1H chemical shifts, $CDCl_3$ (δ , ppm): 2.22–2.31 (m, 4H, CH_2P); 2.71–3.06 (m, 4H, CH_2Ph); 6.21 (m, 1H, H(X)); 6.25 (m, 1H, H(A)); 6.47 (m, 1H, H(B)); 7.17–7.26 (m, 10H, Ph); $^2J_{H(A)H(B)} = 1.3$ Hz, $^3J_{H(A)H(X)} = 11.6$ Hz, $^3J_{H(B)H(X)} = 17.6$ Hz, $^2J_{PH(X)} = 24.6$ Hz, $^3J_{PH(A)} = 45.4$ Hz, $^3J_{PH(B)} = 25.2$ Hz; ^{13}C chemical shifts, $CDCl_3$, (δ , ppm): 29.10 (d, CPh, $^2J_{PC} = 2.2$ Hz), 33.91 (d, CP, $^1J_{PC} = 45.4$ Hz), 126.60 (C_p), 128.30 (C_o), 128.70 (C_o), 128.80 (d, $=CH_2$, $^1J_{PC} = 75.4$ Hz), 137.60 (d, $=CH$, $^2J_{PC} = 2.2$ Hz), 140.6 (d, C_{ipso} , $^3J_{PC} = 15.3$ Hz); ^{31}P chemical shifts, $CDCl_3$, (δ , ppm): 33.26. Calc. for $C_{18}H_{21}PSe$ (%): C, 62.25; H, 6.09; P, 8.92; Se, 22. Found (%): C, 61.82; H, 6.13; P, 9.01; Se, 22.51.

Bis(2-phenethylvinyl)phosphine (10). Light-yellow oil; IR (KBr, cm^{-1}): 465, 492 (δ , CPC), 698 [δ , CH(Ph)], 756 (ν , P-C), 781 [δ , CH(Ph)], 834 (ω , $=CH_2$), 942, 965 (τ , $=CH$), 1009, 1141 [δ , CH(Ph)], 1167 (ν , P=O), 1213 (δ , CH of phenyl rings), 1390 (δ , $=CH_2$), 1453 (δ , CH_2), 1497, 1583 [ν , C=C(Ph)], 1603 [ν , C=C (C=C), C=C(Ph)], 2853, 2863, 2922, 2997 (ν , CH), 3001, 3027, 3062, 3085, 3106 [ν , $=CH_2$, $=CH$ (C=C), C=C(Ph)]; 1H chemical shifts, $CDCl_3$ (δ , ppm): 1.67–1.71 (m, 4H, CH_2P); 2.68–2.74 (m, 4H, CH_2Ph); 6.14 (m, 1H, H(X)); 6.18 (m, 1H, H(A)), 6.58 (m, 1H, H(B)); 7.11–7.25 (m, 10H, Ph); $^2J_{H(A)H(B)} = 2.2$ Hz; $^3J_{H(A)H(X)} = 11.7$ Hz; $^3J_{H(B)H(X)} = 18.4$ Hz; $^2J_{PH(X)} = 5.8$ Hz; $^3J_{PH(A)} = 30.4$ Hz; $^3J_{PH(B)} = 13.1$ Hz; ^{13}C chemical shifts, $CDCl_3$, (δ , ppm): 29.73

(d, CP, $^1J_{PC} = 13.2$ Hz), 32.56 (m, CPh, $^2J_{PC} = 14.0$ Hz), 126.02 (C_p), 127.80 (C_o), 128.10 (d, $=CH_2$, $^2J_{PC} = 19.6$ Hz), 128.40 (C_m), 140.0 (d, $=CH$, $^1J_{PC} = 19.6$ Hz), 143.11 (C_{ipso} , $^3J_{PC} = 10.0$ Hz); ^{31}P chemical shifts, $CDCl_3$, (δ , ppm): -26.80. Calc. for $C_{18}H_{21}P$ (%): C, 80.57; H, 7.89; P, 11.54. Found (%): C, 80.82; H, 7.99; P, 11.21.

Acknowledgements

Financial support from the Russian Foundation for Basic Research (Grant No. 08-03-00021) is acknowledged.

References

- [1] (a) M. S. Rahman, J. W. Steed, K. K. Hii, *Synthesis* **2000**, 9, 1320; (b) A. M. Maj, K. M. Pietrusiewicz, I. Suisse, F. Agbossou, A. Mortreux, *J. Organomet. Chem.* **2001**, 626, 157; (c) M. S. Rahman, M. Oliana, K. K. Hii, *Tetrahedron: Asymmetry* **2004**, 15, 1835; (d) D. V. Griffiths, H. J. Groombridge, P. M. Mahoney, S. P. Swetnam, G. Walton, D. C. York, *Tetrahedron* **2005**, 61, 4595.
- [2] (a) R. K. Haynes, T. L. Au-Yeung, W. K. Chan, W. L. Lam, Z. Y. Li, L. L. Yeung, A. S. C. Chan, P. Li, M. Koen, C. R. Mitchell, S. C. Vonwiller, *Eur. J. Org. Chem.* **2000**, 18, 3205; (b) P. Barbaro, C. Bianchini, G. Giambastiani, A. Togni, *Chem. Commun.* **2002**, 22, 2672; (c) M. Alajarin, C. Lopez-Leonardo, P. Llamas-Lorente, *Lett. Org. Chem.* **2004**, 1, 145; (d) L. B. Han, C. Q. Zhao, *J. Org. Chem.* **2005**, 70, 10121.
- [3] R. T. Paine, E. M. Bond, S. Parveen, N. Donhart, E. N. Duesler, K. A. Smith, H. Noth, *Inorg. Chem.* **2002**, 41, 444.
- [4] For a review, see (a) G. Chelucci, G. Orru, G. A. Pinna, *Tetrahedron* **2003**, 59, 9471; (b) V. V. Grushin, *Chem. Rev.* **2004**, 104, 1629; For recent examples, see; (c) Q. Dai, W. Gao, D. Liu, L. M. Kapes, X. Zhang, *J. Org. Chem.* **2006**, 71, 3928; (d) D. Benito-Garagorri, J. Wiedermann, M. Pollak, K. Mereiter, K. Kirchner, *Organometallics* **2007**, 26, 217.
- [5] (a) S. V. Levchik, E. D. Weil, *Polym. Int.* **2005**, 54, 11; (b) A. Marklund, B. Andersson, P. Haglund, *Environ. Sci. Technol.* **2005**, 39, 3555; (c) G. Ribera, L. A. Mercado, M. Galia, V. Cadiz, *J. Appl. Polym. Sci.* **2006**, 99, 1367; (d) K. Faghihi, K. Zamani, *J. Appl. Polym. Sci.* **2006**, 101, 4263; (e) G. V. Plotnikova, S. F. Malysheva, N. K. Gusarova,

- A. K. Khaliulin, V. P. Udilov, K. L. Kuznetsov, *Russ. J. Appl. Chem.* **2008**, 81, 304.
- [6] (a) F. J. Alguacil, M. Alonso, *Hydrometallurgy* **2004**, 74, 157; (b) D. S. Flett, *Organomet. Chem.* **2005**, 690, 2426; (c) Z. Chan, Y. Yan-Zhao, Z. Tao, H. Jian, L. Chang-Hong, *J. Radioanal. Nucl. Chem.* **2005**, 265, 419.
- [7] (a) S. P. Gubin, N. A. Kataeva, G. B. Khomutov, *Russ. Chem. Bull.* **2005**, 54, 827; (b) H. Liu, J. S. Owen, A. P. Alivisatos, *J. Am. Chem. Soc.* **2007**, 129, 305.
- [8] (a) N. A. Chernysheva, N. K. Gusarova, B. A. Trofimov, *Russ. J. Org. Chem.* **2000**, 36, 11; (b) S. N. Arbuzova, N. K. Gusarova, B. A. Trofimov, *Arkivoc* **2006**, 5, 12.
- [9] Yu. Yu. Rusakov, L. B. Krivdin, N. V. Istomina, V. A. Potapov, S. V. Amosova, *Magn. Reson. Chem.* **2008**, 46, 979.
- [10] L. B. Krivdin, Yu. Yu. Rusakov, E. Yu. Schmidt, A. I. Mikhaleva, B. A. Trofimov, *Aust. J. Chem.* **2007**, 60, 583.
- [11] (a) C. I. Sainz-Díaz, A. Hernández-Laguna, N. J. Smeyers, Y. G. Smeyers, *J. Mol. Struct. THEOCHEM* **1995**, 330, 231; (b) C. I. Sainz-Díaz, A. Hernández-Laguna, Y. G. Smeyers, *J. Mol. Struct. THEOCHEM* **1997**, 390, 127.
- [12] (a) F. J. Meléndez, B. Gallego-Luxan, J. Demaison, Y. G. Smeyers, *J. Comput. Chem.* **2000**, 21, 1167; (b) K. M. Pietrusiewicz, M. Kuźnikowski, W. Wiczorek, A. Brandi, *Heteroatom Chem.* **2004**, 3, 37.
- [13] A. D. Becke, *J. Chem. Phys.* **1993**, 98, 5648.
- [14] C. Lee, W. Yang, R. G. Parr, *Phys. Rev. B* **1988**, 37, 785.
- [15] (a) E. S. Nielsen, P. Jørgensen, J. Oddershede, *J. Chem. Phys.* **1980**, 73, 6238; (b) K. L. Bak, H. Koch, J. Oddershede, O. Christiansen, S. P. A. Sauer, *J. Chem. Phys.* **2000**, 112, 4173; (c) M. J. Packer, E. K. Dalskov, T. Enevoldsen, H. J. Aa. Jensen, J. Oddershede, *J. Chem. Phys.* **1996**, 105, 5886.
- [16] (a) S. P. A. Sauer, *J. Phys. B* **1997**, 30, 3773; (b) T. Enevoldsen, J. Oddershede, S. P. A. Sauer, *Theor. Chem. Acc.* **1998**, 100, 275.
- [17] D. E. Woon, T. H. Dunning Jr, *J. Chem. Phys.* **1993**, 98, 1358.
- [18] (a) T. H. Dunning Jr, *J. Chem. Phys.* **1989**, 90, 1007; (b) R. A. Kendall, T. H. Dunning Jr, R. J. Harrison, *J. Chem. Phys.* **1992**, 96, 6796.
- [19] T. Helgaker, M. Jaszunski, K. Ruud, A. Gorska, *Theor. Chem. Acc.* **1998**, 99, 175.
- [20] P. F. Provasi, G. A. Aucar, S. P. A. Sauer, *J. Chem. Phys.* **2001**, 115, 1324.
- [21] L. B. Krivdin, R. H. Contreras, *Annu. Rep. NMR Spectrosc.* **2007**, 61, 133.
- [22] V. M. S. Gil, W. Philipsborn, *Magn. Reson. Chem.* **1989**, 27, 409.
- [23] (a) P. J. Krueger, J. Jan, H. Wieser, *J. Mol. Struct.* **1970**, 5, 375; (b) F. Bernardi, H. B. Schlegel, S. Wolfe, *J. Mol. Struct.* **1976**, 35, 149; (c) D. C. McKean, *Chem. Soc. Rev.* **1978**, 7, 399; (d) H. D. Thomas, K. Chen, N. L. Allinger, *J. Am. Chem. Soc.* **1994**, 116, 5887; (e) D. G. Zaccari, J. P. Snyder, J. E. Peralta, O. E. Taurian, R. H. Contreras, V. Barone, *Mol. Phys.* **2002**, 100, 705.
- [24] (a) C. Pérez, R. Suardíaz, P. J. Ortiz, R. Crespo-Otero, G. M. Bonetto, J. A. Gavín, J. M. García de la Vega, J. San Fabián, R. H. Contreras, *Magn. Reson. Chem.* **2008**, 46, 846; (b) S. Pedersoli, F. P. dos Santos, R. Rittner, R. H. Contreras, C. F. Tormena, *Magn. Reson. Chem.* **2008**, 46, 202; (c) F. P. dos Santos, C. F. Tormena, R. H. Contreras, R. Rittner, A. Magalhães, *Magn. Reson. Chem.* **2008**, 46, 107; (d) C. F. Tormena, J. D. Vilcachagua, V. Karcher, R. Rittner, R. H. Contreras, *Magn. Reson. Chem.* **2007**, 45, 590.
- [25] M. W. Schmidt, K. K. Baldrige, J. A. Boatz, S. T. Elbert, M. S. Gordon, J. H. Jensen, S. Koseki, N. Matsunaga, K. A. Nguyen, S. J. Su, T. L. Windus, M. Dupuis, J. A. Montgomery, *J. Comput. Chem.* **1993**, 14, 1347.
- [26] R. Krisnan, J. S. Binkley, R. Seeger, J. A. Pople, *J. Chem. Phys.* **1980**, 72, 650.
- [27] Dalton, A Molecular Electronic Structure Program, Release 2.0, see <http://www.kjemi.uio.no/software/dalton/dalton.html>, **2005**.